PAPER

Check for updates

Application of magnetic deep eutectic solvents as an efficient catalyst in the synthesis of new 1,2,3-triazole-nicotinonitrile hybrids *via* a cooperative vinylogous anomeric-based oxidation†

Monireh Navazeni, Mohammad Ali Zolfigol, [iD] * Morteza Torabi and Ardeshir Khazaei*

Magnetic deep eutectic solvents (MDESs) are adjuvants and an emerging subclass of heterogeneous catalysts in organic transformations. Herein, choline chloride (Ch/Cl) embedded on naphthalene bis-urea-supported magnetic nanoparticles, namely, $Fe_3O_4@SiO_2@DES1$, was constructed by a special approach. This compound was scrutinized and characterized by instrumental techniques such as FTIR, thermogravimetry and derivative thermogravimetry (TGA/DTG), field emission scanning electron microscopy (FESEM), energy-dispersive X-ray spectroscopy (EDS), elemental mapping, vibrating sample magnetometer (VSM) and X-ray diffraction (XRD) analyses. Potential catalytic activity of $Fe_3O_4@SiO_2@DES1$ was impressive, facilitating the synthesis of new 1,2,3-triazole-nicotinonitrile hybrids *via* a multicomponent method with 65–98% yields. Enhanced rates, high yields, mild reaction conditions, and recycling and reusability of $Fe_3O_4@SiO_2@DES1$ are the distinct benefits of this catalytic organic synthetic methodology.

Introduction

Deep eutectic solvents (DESs), one of the progressive families of ionic liquids, are composed of binary or ternary mixtures of compounds that can associate mainly *via* hydrogen bond interactions.[1–3] Due to the brilliant, useful, and efficient properties of DESs, these materials are excellent alternatives to conventional organic solvents and classic ionic liquids.[4–6] DESs have easy synthetic routes, and they are biodegradable, cheap and non-flammable.[7] The applications of these materials, including catalytic applications,[8] separation processes,[9] biotechnology,[10] material sciences[11] and environmental protection,[12] have been significantly developed. In recent years, DESs have been widely used in many catalytic transformations.[13–15] Their intrinsic catalytic activity, designability and excellent stability have a robust partnership in catalytic oxidations,[16] CO_2 fixation utilities,[17] multicomponent reactions,[18] desulfurization[19] and coupling reactions.[20] Urea derivatives, as an impactful component of DESs, act as hydrogen bond donors in these systems.[21] Due to the inherent catalytic activity of urea-based compounds as organocatalysts, these moieties enhance the catalytic potential of DESs.[22,23] Very recently, a new class of hybrid DESs, namely, eutectogels, was

reported for the catalytic synthesis of pyridines and chromenes.[24]

Recently, the incorporation of magnetic nanoparticles (MNPs) with DESs to achieve unique heterogeneous catalytic systems has attracted great attention, which have suitable properties for various purposes.[25] Since the recovery and reusability of DESs are problematic, when these compounds are decorated on the surface of MNPs, their defects get resolved.[26] Considering the substantial research carried out on homogeneous DESs, designing and constructing these materials in the heterogeneous phase will endow them with new properties and advantages for their effective performance. Furthermore, heterogeneous DESs will not only retain many of the benefits of homogeneous DESs, but can also be easily separated from the reaction mixture. Considering these distinctions, magnetic DESs is a promising approach in various academic and industrial fields.[27,28] The modification of MNPs by ionic liquids and DESs can enhance their catalytic utilities.[27] Magnetic DESs provide more variations and efficiencies to most of the catalysts. On account of the environmentally friendly nature, high activity, easy recoverability and reusability as well as good stability of heterogeneous DESs, these materials can be robust and fruitful catalysts. In the last years, MNP-decorated DESs were used as heterogeneous catalysts in many organic reactions such as coupling reactions,[28] reduction of aldehydes,[29] and multicomponent reactions.[30,31] Hence, the construction and applications of magnetic DESs have a developing trend and deserve more attention. Several catalytic applications of

Department of Organic Chemistry, Faculty of Chemistry and Petroleum Sciences, Bu-Ali Sina University, Hamedan, Iran. E-mail: zolfi@basu.ac.ir; mzolfigol@yahoo.com; khazaeiardeshir@gmail.com
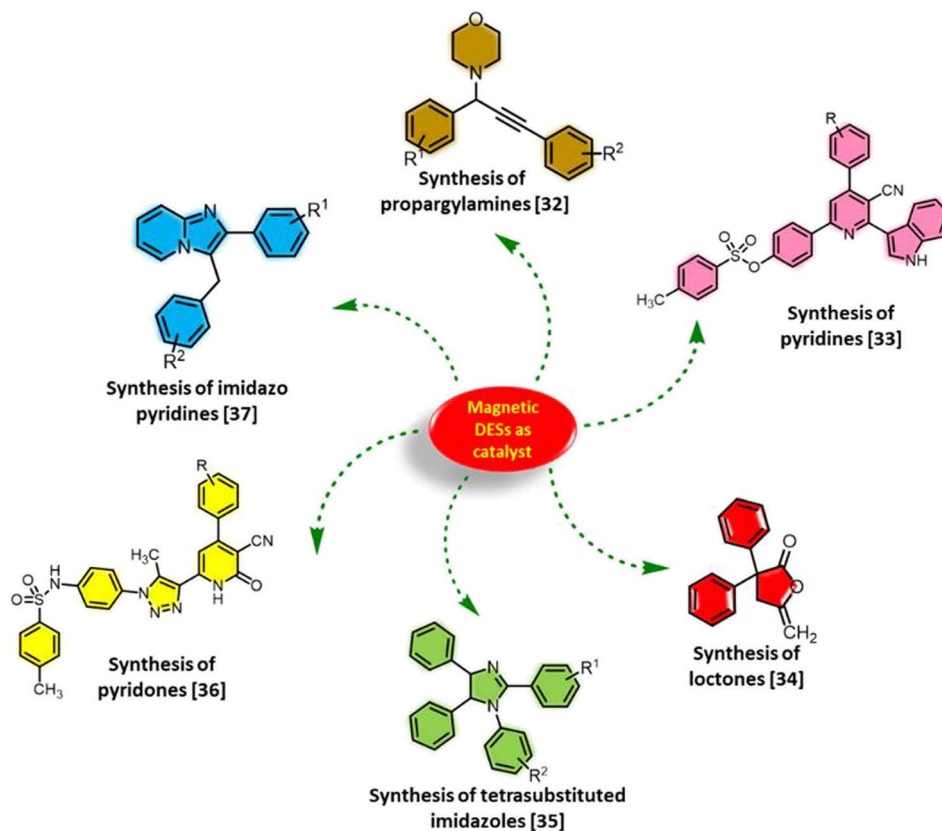
Scheme 1 Several catalytic applications of magnetic DESs in multicomponent reactions.

magnetic DESs in the multicomponent reactions are observed in Scheme 1.

According to the literature, pyridine-containing heterocycles have a brilliant background in many studies such as functional materials, biology, medicinal, agriculture, pharmaceutical molecules, and many miscellaneous areas.[38–40] In an intensive approach, pyridines are widely used in supramolecular chemistry,[41] polymers,[42] coordination chemistry,[43] chemosensors,[44] surfactants,[45] catalysts,[46] organic dyes,[47] *etc.* In addition, fabulous medicinal properties of pyridine cores such as anticancer,[48] anti-inflammatory,[48] anti-Parkinsonian,[49] antidepressant,[50] NADP−NADPH coenzymes[51] and Alzheimer's diseases[52] are interesting. Particularly, N-heterocyclic compounds with the nicotinonitrile moiety are one of the prominent families of pyridines.[53,54] These substrates are present in many drugs. For example, anticancer, antimicrobial, antiproliferative and antihistaminic are only a few of the medicinal properties of these compounds.[55–57] Very recently, the chemistry of the pyridine scaffold and its synthesis and applications as biologically active compound was comprehensively reviewed.[58]

Triazole scaffolds, as another type of N-heterocyclic compound with fundamental and superior applications in vast domains of chemistry such as metal complexes, energetic materials, chemo-sensors, pharmaceuticals, and dyes, have gained significant importance.[59–61] Nevertheless, the most important use of triazoles is their pharmaceutical utilities such as antidepressant,[62] anticancer,[62] antibacterial[63] and antiviral

agents.[64] Recently, hybrid heterocyclic materials, due to their extraordinary properties and synergistic effects in medicinal fields, have been increasingly explored.[65] Due to the synergistic effect of pyridine-triazole hybrids to control the disease agents, much attention has been paid to these materials and several papers have reported on pyridine-triazole hybrids.[66] Nonetheless, the 1,2,3-triazole-nicotinonitrile hybrid deserves more attention.

Considering that the majority of our focus is on the design and synthesis of hybrid pyridines,[67] herein, the catalytic synthesis of a new 1,2,3-triazole-nicotinonitrile hybrid using Fe_3O_4@DES1 as the magnetic DES was investigated (Scheme 2 and 3). Moreover, the role of a cooperative vinylogous anomeric-based oxidation (CVABO) as a stereoelectronic effect in the synthesis of pyridine rings was also studied.[68]

Results and discussion

To the best of our knowledge, pyridine is one of the most famous scaffolds that is present as the structural core of various chemical, biological, and medicinal heterocycles and natural products. The intrinsic chemical and physical properties of pyridine make it a suitable core to prepare a wide range of suitable derivatives, including vitamins, dyes, agrochemicals, pesticides, adhesives, and biologically active compounds. Singh has published a book entitled "Recent Developments in the Synthesis and Application of Pyridines" with the collaboration
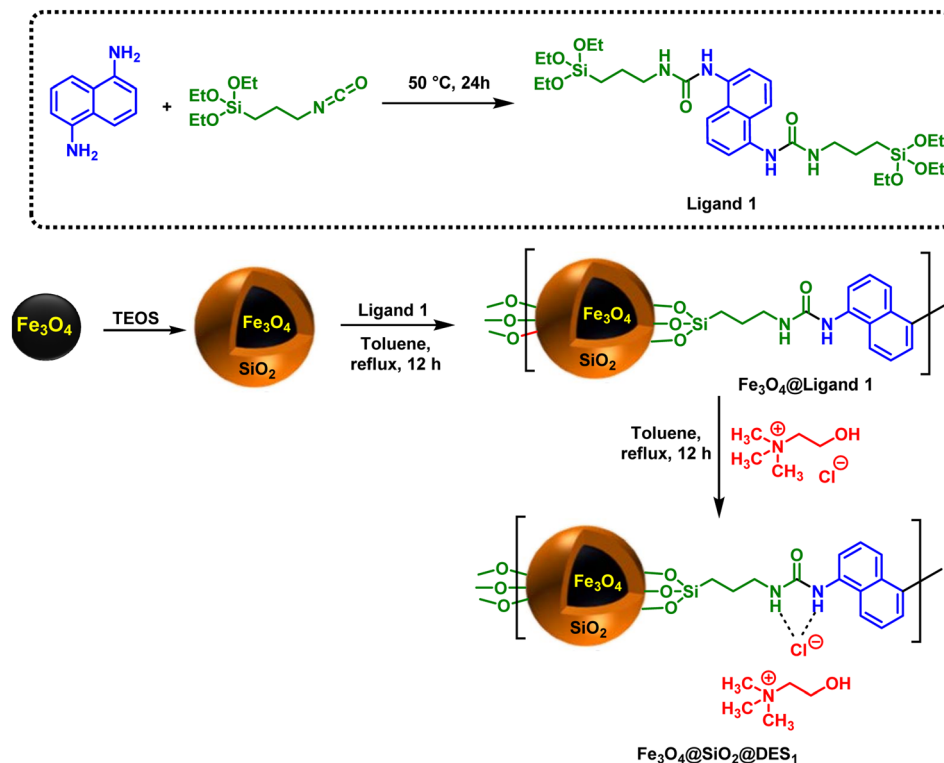
Scheme 2 Schematic of Fe₃O₄@SiO₂@DES1 synthesis.

of other authors such as us.[48] In continuation of our pervious investigation on the synthesis of hybrid pyridines,[60,64,65] we decided to design, synthesize and apply Fe₃O₄@SiO₂@DES1 for

the catalytic preparation of a new category of pyridine derivatives. At first, the characterization of the described catalyst will be discussed.
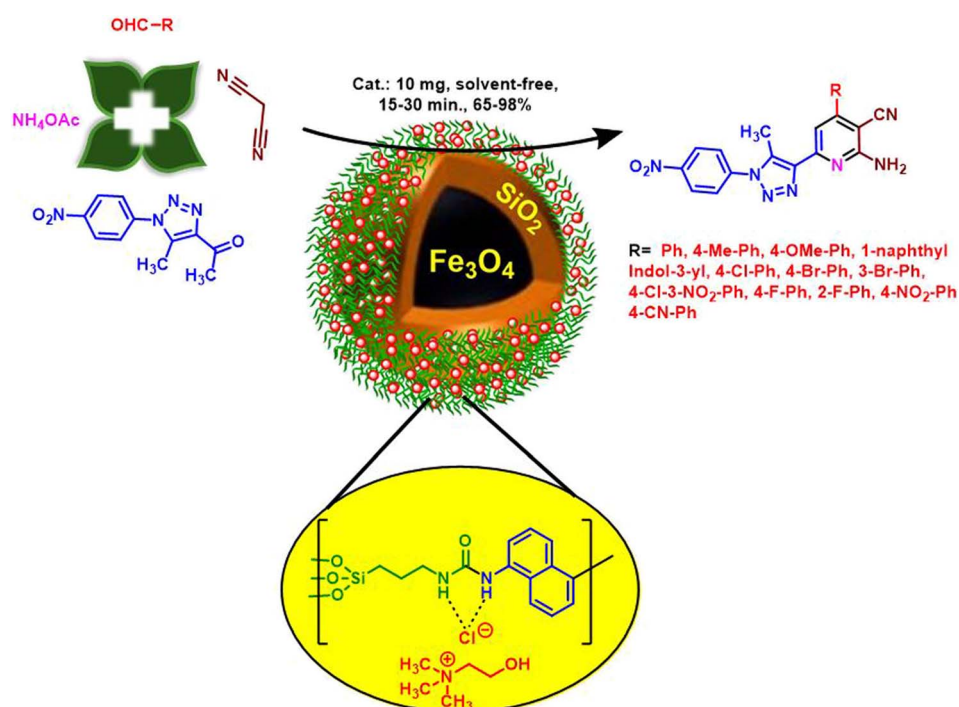
Scheme 3 Illustration of the synthesis of 1,2,3-triazole-nicotinonitrile derivatives.

The synthesized $Fe_3O_4@SiO_2@DES1$ was precisely characterized by several instrumental methodologies including FTIR, EDS, mapping, FESEM, VSM and XRD. FTIR spectroscopy were used to approve the chemical structure of $Fe_3O_4@SiO_2@DES1$ and its related intermediate. In the FTIR spectrum of $Fe_3O_4@SiO_2$ (Fig. 1), the characteristic peaks of Fe–O, Si=O and free hydroxy groups are obtained at 586, 1111 and 3378 cm^{-1}, respectively. In the FTIR spectrum of Ligand 1, strong peaks are shown at 3306, 1626 and 1576 cm^{-1} arising from the NH, C=O and C=C stretching bands, respectively. The C=O and C=C stretching vibration for $Fe_3O_4@SiO_2@Ligand\ 1$ appeared at 1634 and 1540 cm^{-1}, respectively, and these confirm that the Ligand 1 is successfully supported at the $Fe_3O_4@SiO_2$ surface. Similarly, in the FTIR spectrum of $Fe_3O_4@SiO_2@DES1$, the characteristic peaks at 1635 and 1534 confirm the successful synthesis of the catalyst.

EDS/mapping is a key analysis to show the successful construction of the DES system. The presence of Ch/Cl on the surface of $Fe_3O_4@SiO_2$ (Cl as key part of DES) was confirmed by

EDS/mapping analyses. Anyway, the presence and uniform distribution of other expected elements including Fe, Si, O, C and N related to previous steps of catalyst synthesis were well confirmed by the EDS signals and mapping images of $Fe_3O_4@SiO_2@DES1$ (Fig. 2).

FESEM images were used to investigate the morphology and size of the synthesized catalyst. These images revealed that $Fe_3O_4@SiO_2@DES1$ has uniform spherical morphology, and these particles are in the size range of 26–44 nm. The magnetic nature of the catalyst leads to the creation of interwoven single spherical particles with sizes smaller than 40 nm (Fig. 3). In addition, the crystalline structure of $Fe_3O_4@SiO_2@DES1$ was investigated by XRD analysis. The characteristic signals at 30, 35, 43, 53, 57 and 62° for the catalyst correspond to the cubic geometry for Fe_3O_4. The broad peak at 20–25° is related to the SiO_2 groups Moreover, a decrease in the intensity of peaks for $Fe_3O_4@SiO_2@DES1$ compared to Fe_3O_4 is because of the presence of the organic and inorganic layers on the surface of Fe_3O_4.
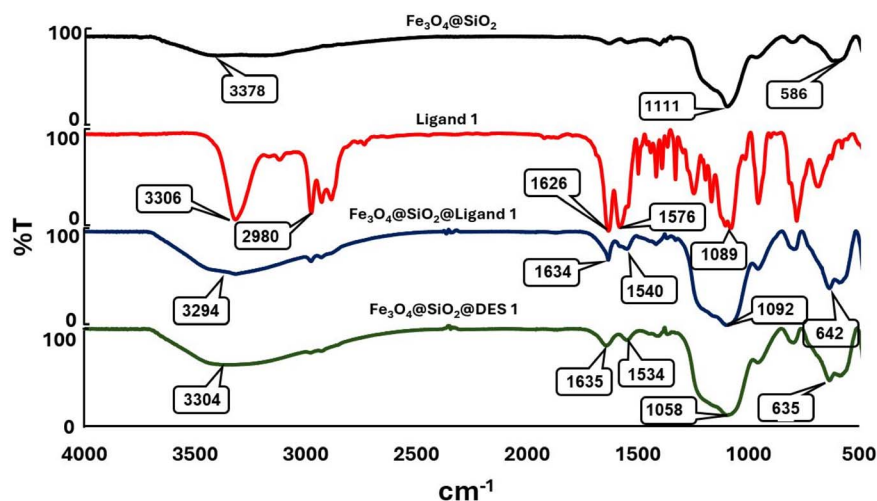

Fig. 1 FTIR spectra of $Fe_3O_4@SiO_2$, Ligand 1, $Fe_3O_4@SiO_2@Ligand\ 1$ and $Fe_3O_4@SiO_2@DES1$.
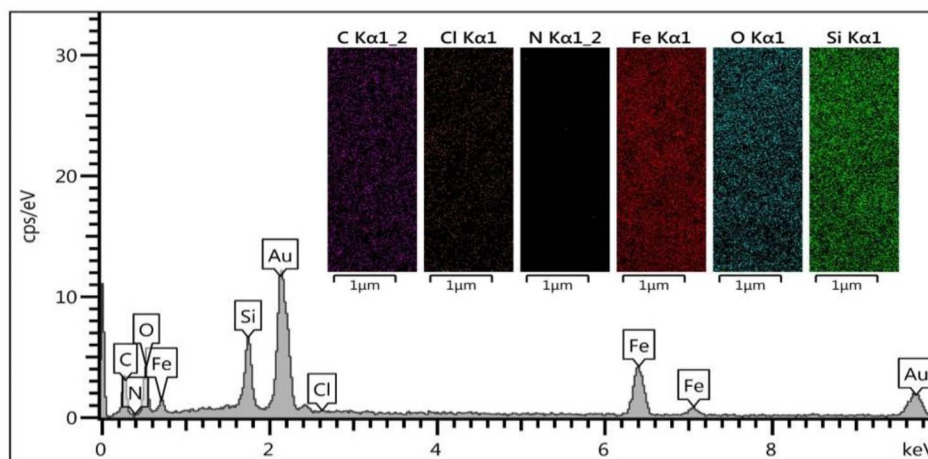
Fig. 2 EDS/mapping analyses of $Fe_3O_4@SiO_2@DES1$
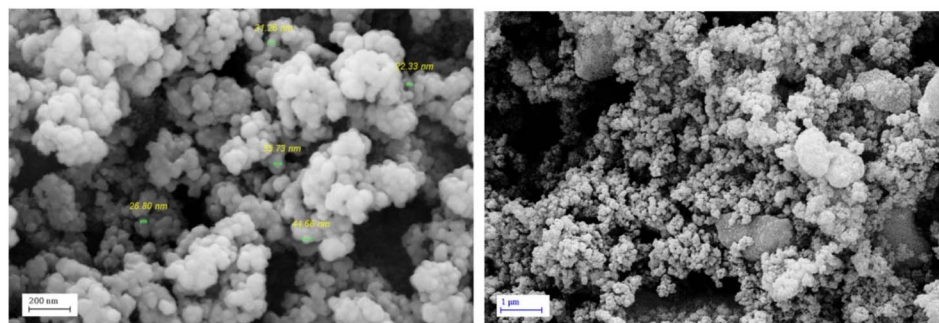
Fig. 3 FESEM images of $Fe_3O_4@SiO_2@DES1$

Nonetheless, after the decoration of $Fe_3O_4@SiO_2$ by organic layers, its geometry is preserved (Fig. 4).

In another study, VSM analysis was achieved from Fe_3O_4, $Fe_3O_4@SiO_2$, and $Fe_3O_4@SiO_2@DES1$ for the determination of their magnetic properties. The magnetic value of the described catalyst is 7.2 emu g^{-1}, which is significantly less than the magnetic value of Fe_3O_4 and $Fe_3O_4@SiO_2$. Based on the achieved data, the organic layers are well supported on the surface of magnetic cores and $Fe_3O_4@SiO_2@DES1$ has a considerable magnetic value (Fig. 5). TGA analysis indicates that $Fe_3O_4@SiO_2@DES1$ can be stable up to 325 °C and retain 80% of its initial mass even at 600 °C under N_2. The first weight loss in the range of 325–383 °C is related to the removal of Ch/Cl,[69] and the second weight loss at 513 °C is because of the decomposition of organic layers, which is linked to surface of $Fe_3O_4@SiO_2$ by covalent bonds (Fig. 6).

After the characterization of $Fe_3O_4@SiO_2@DES1$, it was used as a heterogeneous catalyst for the synthesis of new 1,2,3-triazole-nicotinonitrile hybrids. To improve the methodology of the synthesis of $Fe_3O_4@SiO_2@DES1$, the effects of the temperature, solvent and amount of catalyst were explored. For this goal, the synthesis of **1f** molecule was used as a model reaction (Table 1). With respect to the influence of the temperature, several temperatures were applied for the synthesis of **1f**.
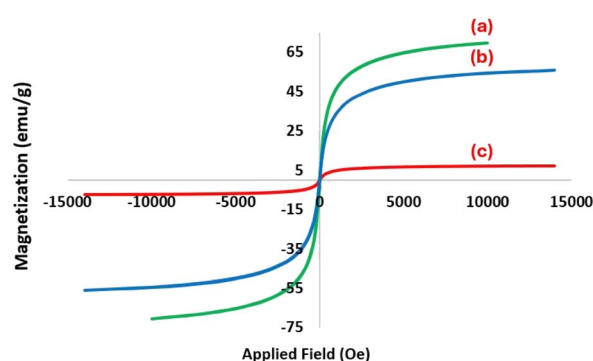

Fig. 5 VSM curves of Fe_3O_4 (a), $Fe_3O_4@SiO_2$ (b) and $Fe_3O_4@SiO_2@DES1$ (c).
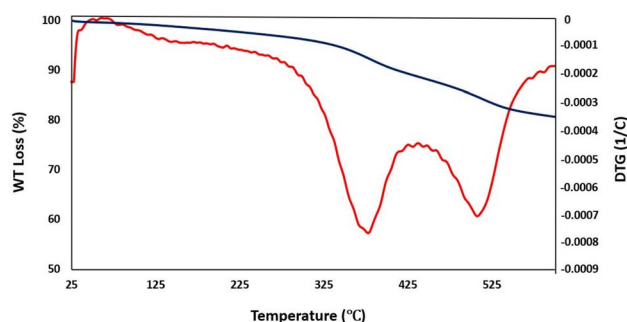
Fig. 6 TGA/DTG curves of $Fe_3O_4@SiO_2@DES1$.

According to the obtained results, 120 °C was selected as the optimum temperature. With respect to the influence of the solvent, the model reaction was done under solvent-free and reflux conditions. Several solvents such as CH_3OH, $CHCl_3$, EtOAc, acetone, CH_3CN, and EtOH were used, but solvent-free conditions gave the best result. Finally, the amount of the catalyst was examined, wherein 10 mg of the catalyst was selected as the optimum value.

In continuation, we are interested in developing the generality of catalytic performance of $Fe_3O_4@SiO_2@DES1$ for the synthesis of a new library of 1,2,3-triazole-nicotinonitrile hybrids. Hence, several aromatic aldehydes bearing electron-withdrawing and electron-releasing substituents were used for

Fig. 4 XRD patterns of (a) Fe_3O_4 and (b) $Fe_3O_4@SiO_2@DES1$

Table 1 Optimization of reaction conditions for the synthesis of **1f**[a]

Entry	Solvent	Catalyst loading (mg)	Temperature (°C)	Time (min)	Yield[b] (%)
1	—	5	130	20	78
2	—	**10**	**120**	**20**	**94**
3	—	20	120	20	94
4	—	—	120	60	52
5	—	10	120	30	54
6	—	10	90	30	46
10	CH_3OH	10	Reflux	60	88
11	$CHCl_3$	10	Reflux	60	64
12	EtOAc	10	Reflux	60	72
13	Acetone	10	Reflux	60	56
14	CH_3CN	10	Reflux	60	50
15	EtOH	10	Reflux	60	78

[a] Reaction conditions: 4-chlorobenzaldehyde (1 mmol, 0.14 g), 1-(5-methyl-1-(4-nitrophenyl)-1H-1,2,3-triazol-4-yl)ethan-1-one (1 mmol, 0.246 g), malononitrile (1 mmol, 0.066 g); ammonium acetate (1.5 mmol, 0.078 g). [b] Isolated yield.

this purpose. The achieved products were synthesized in the clean reaction and have high yield as well as short reaction times (Table 2).

To explore the important role of the components of Fe_3O_4@SiO_2@DES1, the **1f** molecule was synthesized using Fe_3O_4, Fe_3O_4@SiO_2, Ch/Cl and Ligand 1 was compared to Fe_3O_4@SiO_2@DES1. According to the obtained results, each of these components can have a catalytic role to some extent. The free hydroxy groups on the surface of Fe_3O_4 and Fe_3O_4@SiO_2 have significant catalytic activity, and the ionic structure of Ch/Cl enhances its catalytic performance. Moreover, urea segments in Ligand 1 can act as a hydrogen-bonding catalyst. Therefore, the synergistic effects of these parts can improve the catalytic potential of Fe_3O_4@SiO_2@DES1 (Table 3).

Scheme 4 exhibits the suggested mechanism for the synthesis of 1,2,3-triazole-nicotinonitrile hybrids using Fe_3O_4@SiO_2@DES1 catalyst. The Knoevenagel reaction using activated benzaldehyde and malononitrile as the starting materials yields intermediate **a**. Besides, ammonia, derived from the *in situ* dissociation of ammonium acetate, reacts with 1-(5-methyl-1-(4-nitrophenyl)-1H-1,2,3-triazol-4-yl)ethan-1-one and intermediate **b** is produced. Hereafter, these intermediates thus formed undergo condensation reaction to yield intermediate **c**. Then, due to the intramolecular nucleophilic attack and tautomerization processes, intermediate **f** was performed. Then, the final product was achieved *via* the cooperative vinylogous anomeric-based oxidation (CVABO)[66–68,70] of dihydropyridine intermediates and their conversion to the corresponding pyridines.

The recycling and reusability of Fe_3O_4@SiO_2@DES1 was investigated using the model reaction. After running the model

reaction each time, the reaction mixture was dissolved in DMF, and the catalyst was separated by an external magnet and washed with EtOH three times. The separated catalyst was dried and used the next time. Finally, it was found that the catalyst can be recovered and reused up to 5 times, and a slight drop in yield of the product is observed (Fig. 7). The recovered catalyst was characterized using several methods such as XRD, EDS/mapping and FESEM analyses (see in the ESI†).

Experimental section

The required precursors were synthesized according to our recently reported educational synthetic organic theory.[71]
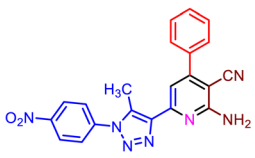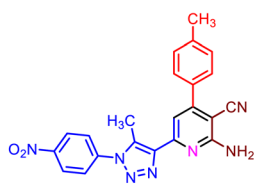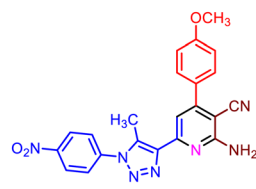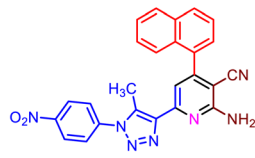
Synthesis of Ligand 1
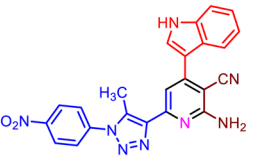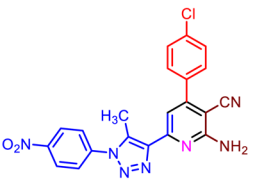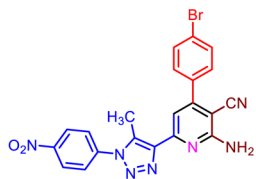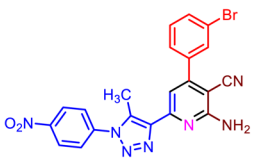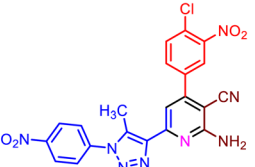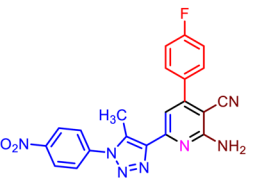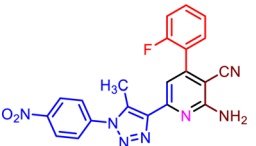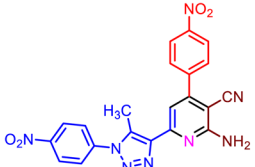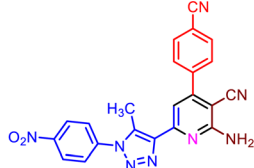
Initially, naphthalene-1,5-diamine (1 mmol, 0.158 g) and triethoxy(3-isocyanatopropyl)silane (2 mmol, 0.495 g) were added to a 10 mL round-bottomed flask and stirred under solvent-free condition at 50 °C for 24 h. After that, the white solid that appeared was washed with a mixture of *n*-hexane and EtOAc (5/1, v/v) to give a pure product.

Synthesis of Fe_3O_4@SiO_2@DES1

First and foremost, Fe_3O_4@SiO_2 was prepared according to the previously reported synthetic method.[72] Then, 1 g of Fe_3O_4@SiO_2, Ligand 1 (2 mmol, 0.652 g) and 90 mL of dry toluene were poured into a 100 mL round-bottomed flask and sonicated for 15 min. Then, it was refluxed for 48 h at 110 °C. The remaining solid was separated by an external magnet and washed with EtOH. The separated precipitate was dried to yield

Table 2 Synthesis of 1,2,3-triazole-nicotinonitrile hybrids in the presence of Fe$_3$O$_4$@SiO$_2$@DES1 as a catalyst[a]

1a, 15min.: 90%
M.p.:233-235 °C

1b, 25 min.:70%
M.p.: 215-217 °C

1c,20 min.: 85%
M.p.: 270-271 °C

1d, 15 min.: 88%
M.p.: 266-270 °C

1e, 20 min.:87%
M.p.: >300 °C

1f, 20 min.: 94%
M.p.: 294-297°C

1g, 15 min.: 96%
M.p.: >300 °C

1h, 15 min.:80%
M.p.: 233-235°C

1i, 30 min.:98%
M.p.: > 300 °C

1j, 15 min.: 92%
M.p.: 251-255 °C

1k, 20 min.: 65%
M.p.: 206-209 °C

1l, 15 min.: 90%
M.p.: 266-268 °C

1m, 15 min.: 95%
M.p.: > 300 °C

[a] Reaction conditions: aldehyde (1 mmol), 1-(5-methyl-1-(4-nitrophenyl)-1H-1,2,3-triazol-4-yl)ethan-1-one (1 mmol, 0.246 g), malononitrile (1 mmol, 0.066 g), ammonium acetate (1.5 mmol, 0.078 g), solvent-free, 120 °C, catalyst = 10 mg, reported yields refer to the isolated yields.

Table 3 Investigation of the catalytic performance of Fe$_3$O$_4$@SiO$_2$@DES1 compared to Fe$_3$O$_4$, Fe$_3$O$_4$@SiO$_2$, Ligand 1 and Ch/Cl upon the preparation of **1f**[a]

Entry	Catalyst	Load of catalyst	Yield (%)
1	Fe$_3$O$_4$@SiO$_2$@DES1	10 mg	94
2	Fe$_3$O$_4$	10 mg	30
3	Fe$_3$O$_4$@SiO$_2$	10 mg	40
4	Ligand 1	10 mol%	35
	Ch/Cl	10 mol%	50

[a] Reaction conditions: 4-Cl-benzaldehyde (1 mmol, 0.14 g), 1-(5-methyl-1-(4-nitrophenyl)-1H-1,2,3-triazol-4-yl)ethan-1-one (1 mmol, 0.246 g), malononitrile (1 mmol, 0.066 g); ammonium acetate (1.5 mmol, 0.078 g). Solvent-free, 120 °C.

Fe$_3$O$_4$@SiO$_2$@Ligand 1. In the next step, 1 g of Fe$_3$O$_4$@SiO$_2$@-Ligand 1, Ch/Cl (4 mmol, 0.56 g) and 50 mL toluene were mixed into a 100 mL round-bottomed flask and again refluxed for 12 h. Finally, Fe$_3$O$_4$@SiO$_2$@DES1 was separated by an external magnet. The separated solid was washed with EtOH and dried at 80 °C.

Synthesis of 1,2,3-triazole-nicotinonitrile hybrids in the presence of Fe$_3$O$_4$@SiO$_2$@DES1

In the first step, 1-(5-methyl-1-(4-nitrophenyl)-1H-1,2,3-triazol-4-yl)ethan-1-one was prepared according to the literature.[73] Then, the aryl aldehyde derivatives (1 mmol), 1-(5-methyl-1-(4-nitrophenyl)-1H-1,2,3-triazol-4-yl)ethan-1-one (1 mmol, 0.246 g), malononitrile (1 mmol, 0.066 g) and ammonium acetate (1.5 mmol, 0.078 g) were mixed into a 10 mL round bottomed

Paper
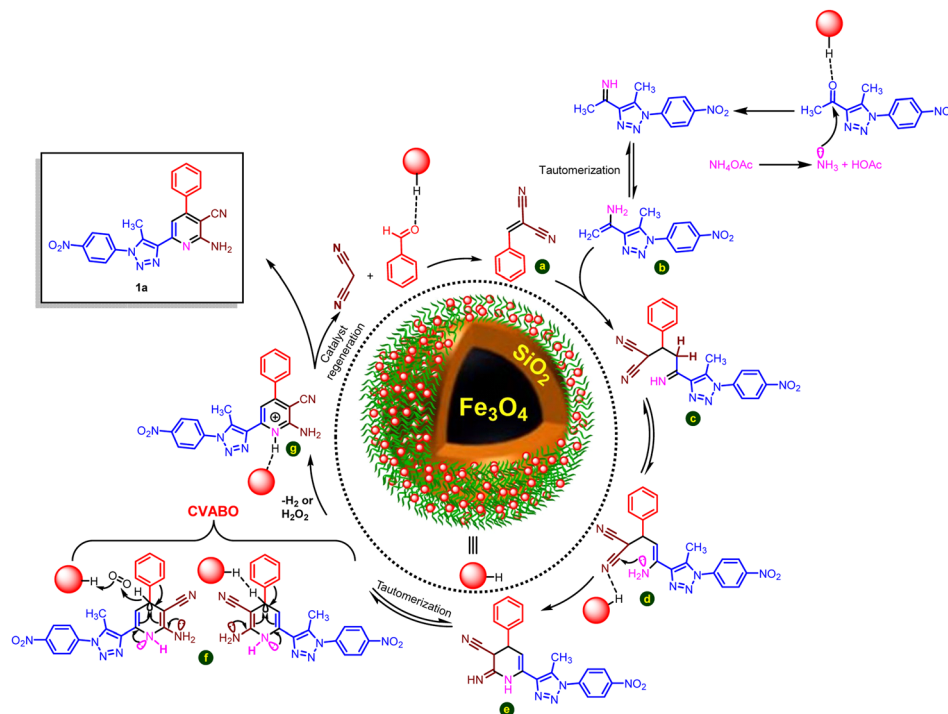
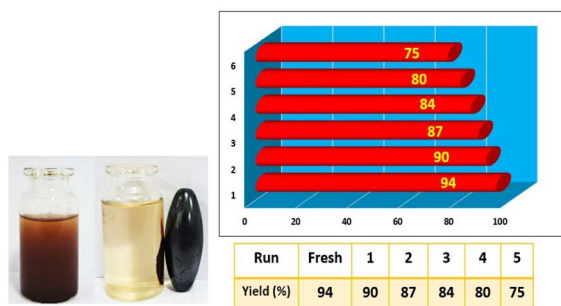**Scheme 4** Suggested mechanistic route for the synthesis of 1,2,3-triazole-nicotinonitrile hybrids.

Fig. 7 Recycling and reusability test of Fe$_3$O$_4$@SiO$_2$@DES1 upon model reaction.

flask containing 10 mg Fe$_3$O$_4$@SiO$_2$@DES1 as the catalyst and stirred vigorously under solvent-free conditions at 120 °C. At the end of the reaction, the catalyst was separated from the reaction mixture using DMF. Then, cold water was added to the DMF solution containing organic compounds, which led to the appearance of a bulk solid. Finally, the desired products were purified by recrystallization in 10 mL acetonitrile.

Spectral data

1,1′-(Naphthalene-1,5-diyl)bis(3-(3-(triethoxysilyl)propyl) urea) (Ligand 1). FTIR (KBr, ν, cm^{-1}): 3317, 2928, 1633, 1581, 1497, 1103, 1079. ^{1}H NMR (400 MHz, DMSO$_{d6}$) δ_{ppm} 8.43 (s, 2H), 8.00 (d, $J = 8$ Hz, 2H), 7.71 (d, $J = 8$ Hz, 2H), 7.44 (t, $J = 8$ Hz, 2H), 6.63 (t, $J = 5.8$ Hz, 2H), 3.77 (q, $J = 7.0$ Hz, 12H), 3.12 (q, $J = 8$ Hz, 4H), 1.56–1.47 (m, 4H), 1.16 (t, $J = 8$ Hz, 18H), 0.63–0.59 (m, 4H).

2-Amino-6-(5-methyl-1-(4-nitrophenyl)-1H-1,2,3-triazol-4-yl)-4-phenylnicotinonitrile (1a). M.p. = 233–235 °C, FTIR (KBr, ν, cm^{-1}): 3495, 3371, 2213, 1625, 1584, 1348. ^{1}H NMR (400 MHz, DMSO$_{d6}$) δ_{ppm} 8.50 (d, $J = 8$ Hz, 2H), 8.05–8.03 (m, 3H), 7.68–7.58 (m, 4H), 7.46 (s, 1H), 7.17 (s, 2H), 2.85 (s, 3H). ^{13}C NMR (101 MHz, DMSO$_{d6}$) δ_{ppm} 160.9, 154.6, 153.4, 147.7, 141.8, 140.4, 136.8, 135.3, 129.7, 128.9, 128.1, 126.4, 125.1, 116.9, 108.9, 86.1, 10.5. MS (m/z) = calcd for C$_{21}$H$_{15}$N$_7$O$_2$: 397.40, found: 398.219.

2-Amino-6-(5-methyl-1-(4-nitrophenyl)-1H-1,2,3-triazol-4-yl)-4-(p-tolyl) nicotinonitrile (1b). M.p. = 215–217 °C, FTIR (KBr, ν, cm^{-1}): 3505, 3381, 2209, 1728, 1614, 1590, 1350. ^{1}H NMR (400 MHz, DMSO$_{d6}$) δ_{ppm} 8.50 (d, $J = 8$ Hz, 2H), 8.04 (d, $J = 12$ Hz, 2H), 7.57 (d, $J = 12$ Hz, 2H), 7.44 (s, 1H), 7.39 (d, $J = 8$ Hz, 2H), 7.13 (s, 2H), 2.83 (s, 3H), 2.42 (s, 3H). MS (m/z) = calcd for C$_{22}$H$_{17}$N$_7$O$_2$: 411.42, found: 412.242.

2-Amino-6-(5-methyl-1-(4-nitrophenyl)-1H-1,2,3-triazol-4-yl)-4-(4-methoxyphenyl) nicotinonitrile (1c). M.p. = 270–271 °C, FTIR (KBr, ν, cm^{-1}): 3505, 3395, 2209, 1603, 1558, 1345. ^{1}H NMR (400 MHz, DMSO$_{d6}$) δ_{ppm} 8.51 (broad peak, 2H), 8.10–7.96 (m, 2H), 7.65 (s, 2H), 7.45 (s, 1H), 7.25–6.99 (m, 4H), 3.87 (s, 3H), 2.85 (d, $J = 8.2$ Hz, 3H). ^{13}C NMR (101 MHz, DMSO$_{d6}$) δ_{ppm} 161.0, 154.2, 153.2, 147.7, 141.8, 135.1, 131.6, 129.7, 128.9, 126.4, 126.3, 125.1, 117.2, 114.3, 108.7, 85.8, 55.3, 10.5. MS (m/z) = calcd for C$_{22}$H$_{17}$N$_7$O$_3$: 427.42, found: 427.300.

2-Amino-6-(5-methyl-1-(4-nitrophenyl)-1H-1,2,3-triazol-4-yl)-4-(naphthalen-1-yl)nicotinonitrile (1d). M.p. = 266–270 °C, FTIR (KBr, ν, cm^{-1}): 3501, 3399, 2209, 1610, 1565, 1523, 1338. ^{1}H NMR (400 MHz, DMSO$_{d6}$) δ_{ppm} 8.50 (d, $J = 8$ Hz, 2H), 8.13–8.03 (m, 4H), 7.70–7.56 (m, 5H), 7.22 (s, 2H), 2.88 (s, 3H). ^{13}C NMR (101 MHz, DMSO$_{d6}$) δ_{ppm} 160.42, 154.0, 153.1, 147.7,

141.8, 140.3, 135.4, 134.7, 133.1, 129.9, 129.4, 128.6, 127.1, 126.6, 126.5, 126.4, 125.5, 125.1, 124.5, 116.3, 112.4, 110.5, 88.6, 10.5. MS (m/z) = calcd for $C_{25}H_{17}N_7O_2$: 447.46, found: 447.000.

2-Amino-4-(1H-indol-3-yl)-6-(5-methyl-1-(4-nitrophenyl)-1H-1,2,3-triazol-4-yl)nicotinonitrile (1e). M.p. > 300 °C FTIR (KBr, ν, cm^{-1}): 3353, 3205, 2210, 1662, 1590, 1422, 1344. ^{1}H NMR (400 MHz, DMSO$_{d6}$) δ_{ppm} 11.88 (s, 1H), 8.53 (broad peak, 4H), 8.30 (s, 1H), 8.11 (broad peak, 4H), 7.57 (s, 1H), 7.28 (s, 2H), 2.88 (s, 3H). ^{13}C NMR (101 MHz, DMSO$_{d6}$) δ_{ppm} 158.4, 151.1, 147.6, 145.1, 143.5, 140.6, 137.1, 133.3, 126.6, 126.3, 125.1, 124.6, 122.1, 120.7, 118.9, 116.3, 112.8, 112.6, 86.5, 10.6.

2-Amino-4-(4-chlorophenyl)-6-(5-methyl-1-(4-nitrophenyl)-1H-1,2,3-triazol-4-yl)nicotinonitrile (1f). M.p. = 294–297 °C, FTIR (KBr, ν, cm^{-1}): 3490, 3358, 2220, 1636, 1590, 1526, 1346. ^{1}H NMR (400 MHz, DMSO$_{d6}$) δ_{ppm} 8.50 (d, J = 8 Hz, 2H), 8.03 (d, J = 8 Hz, 2H), 7.72–7.65 (m, 4H), 7.45 (s, 1H), 7.21 (s, 2H), 2.84 (s, 3H). ^{13}C NMR (101 MHz, DMSO$_{d6}$) δ_{ppm} 160.8, 153.5, 153.3, 147.7, 141.7, 140.4, 135.6, 135.3, 134.6, 130.1, 128.9, 126.4, 125.1, 116.7, 108.8, 85.9, 10.5. MS (m/z) = calcd for $C_{21}H_{14}ClN_7O_2$: 431.84, found: 432.200.

2-Amino-4-(4-bromophenyl)-6-(5-methyl-1-(4-nitrophenyl)-1H-1,2,3-triazol-4-yl)nicotinonitrile (1g). M.p. > 300 °C, FTIR (KBr, ν, cm^{-1}): 3489, 3358, 2219, 1634, 1590, 1524, 1348. ^{1}H NMR (400 MHz, DMSO$_{d6}$) δ_{ppm} 8.50 (d, J = 8 Hz, 2H), 8.04 (d, J = 8 Hz, 2H), 7.80 (d, J = 8 Hz, 2H), 7.64 (d, J = 8 Hz, 2H), 7.45 (s, 1H), 7.21 (s, 2H), 2.84 (s, 3H). ^{13}C NMR (101 MHz, DMSO$_{d6}$) δ_{ppm} 160.8, 153.5, 153.4, 147.7, 141.7, 140.4, 1356.0, 135.3, 131.9, 130.3, 126.4, 125.1, 123.3, 116.7, 108.7, 85.8, 10.5. MS (m/z) = calcd for $C_{21}H_{14}BrN_7O_2$: 476.29, found: 477.700.

2-Amino-4-(3-bromophenyl)-6-(5-methyl-1-(4-nitrophenyl)-1H-1,2,3-triazol-4-yl)nicotinonitrile (1h). M.p. = 233–235 °C, FTIR (KBr, ν, cm^{-1}): 3455, 3384, 2209, 1609, 1588, 1502, 1344. ^{1}H NMR (400 MHz, DMSO$_{d6}$) δ_{ppm} 8.50 (d, J = 8 Hz, 2H), 8.04 (d, J = 8 Hz, 2H), 7.87 (s, 1H), 7.78 (d, J = 8 Hz, 1H), 7.68 (d, J = 8 Hz, 1H), 7.55 (t, J = 8 Hz, 1H), 7.45 (s, 1H), 7.23 (s, 2H), 2.84 (s, 3H). ^{13}C NMR (101 MHz, DMSO$_{d6}$) δ_{ppm} 160.8, 153.5, 152.9, 147.7, 141.7, 140.4, 139.1, 135.3, 132.5, 131.0, 130.7, 127.4, 126.4, 125.1, 121.9, 116.6, 108.9, 86.0, 10.5. MS (m/z) = calcd for $C_{21}H_{14}BrN_7O_2$: 476.29, found: 477.100.

2-Amino-4-(4-chloro-3-nitrophenyl)-6-(5-methyl-1-(4-nitro-phenyl)-1H-1,2,3-triazol-4-yl)nicotinonitrile (1i). M.p. > 300 °C, ^{1}H NMR (400 MHz, DMSO$_{d6}$) δ_{ppm} 8.50 (d, J = 12 Hz, 2H), 8.41 (s, 1H), 8.05–8.01 (m, 4H), 7.53 (s, 1H), 7.31 (s, 2H), 2.84 (s, 3H). ^{13}C NMR (101 MHz, DMSO$_{d6}$) δ_{ppm} 160.7, 153.8, 151.2, 147.8, 147.7, 141.6, 140.3, 136.9, 135.5, 133.5, 132.1, 126.4, 126.1, 126.0, 125.4, 125.1, 116.4, 108.8, 85.8, 40.0, 39.9, 39.6, 39.4, 39.2, 39.0, 38.8, 10.5. MS (m/z) = calcd for $C_{21}H_{13}ClN_8O_4$: 476.84, found: 477.400.

2-Amino-4-(4-florophenyl)-6-(5-methyl-1-(4-nitrophenyl)-1H-1,2,3-triazol-4-yl)nicotinonitrile (1j). M.p. = 251–255 °C, FTIR (KBr, ν, cm^{-1}): 3496, 3377, 2213, 1632, 1588, 1561, 1347. ^{1}H NMR (400 MHz, DMSO$_{d6}$) δ_{ppm} 8.50 (d, J = 8 Hz, 2H), 8.04 (d, J = 8 Hz, 2H), 7.76–7.73 (m, 2H), 7.45–7.41 (m, 3H), 7.19 (s, 2H), 2.84 (s, 3H). ^{13}C NMR (101 MHz, DMSO$_{d6}$) δ_{ppm} 160.8, 153.6, 153.4, 147.7, 141.8, 140.4, 138.0, 135.3, 130.6, 130.5, 126.4, 125.1, 117.9, 116.0, 115.8, 108.9, 95.3, 10.4. MS (m/z) = calcd for $C_{21}H_{14}FN_7O_2$: 415.39, found: 415.900.

2-Amino-4-(2-florophenyl)-6-(5-methyl-1-(4-nitrophenyl)-1H-1,2,3-triazol-4-yl)nicotinonitrile (1k). M.p. = 206–209 °C, FTIR (KBr, ν, cm^{-1}): 3494, 3358, 2222, 1628, 1584, 1520, 1257. ^{1}H NMR (400 MHz, DMSO$_{d6}$) δ_{ppm} 8.50 (d, J = 8 Hz, 2H), 8.04 (d, J = 8 Hz, 2H), 7.65–7.58 (m, 2H), 7.48–7.40 (m, 3H), 7.21 (s, 2H), 2.84 (s, 3H). ^{13}C NMR (101 MHz, DMSO$_{d6}$) δ_{ppm} 160.3, 159.7, 157.3, 153.5, 149.3, 147.7, 141.6, 140.3, 135.4, 132.0, 131.9, 130.7, 126.4, 125.1, 124.6, 124.4, 116.2, 116.0, 109.7, 87.6, 10.4. MS (m/z) = calcd for $C_{21}H_{14}FN_7O_2$: 415.39, found: 416.031.

2-Amino-6-(5-methyl-1-(4-nitrophenyl)-1H-1,2,3-triazol-4-yl)-4-(4-nitrophenyl)nicotinonitrile (1l). M.p. = 266–268 °C, FTIR (KBr, ν, cm^{-1}): 3482, 3367, 2208, 1613, 1562, 1527, 1347. ^{1}H NMR (400 MHz, DMSO$_{d6}$) δ_{ppm} 8.52–8.41 (m, 4H), 8.16–7.90 (m, 4H), 7.54 (s, 1H), 7.30 (s, 2H), 2.85 (s, 3H). ^{13}C NMR (101 MHz, DMSO$_{d6}$) δ_{ppm} 160.8, 153.8, 152.3, 147.9, 147.7, 140.3, 138.2, 135.4, 134.9, 130.6, 126.4, 125.1, 123.0, 116.5, 108.9, 85.9, 10.5. MS (m/z) = calcd for $C_{21}H_{14}N_8O_4$: 442.40, found: 442.000.

2-Amino-4-(4-cyanophenyl)-6-(5-methyl-1-(4-nitrophenyl)-1H-1,2,3-triazol-4-yl)nicotinonitrile (1m). M.p. > 300 °C, FTIR (KBr, ν, cm^{-1}): 3482, 3368, 2229, 2219, 1636, 1589, 1527, 1503, 1406, 1311. ^{1}H NMR (400 MHz, DMSO$_{d6}$) δ_{ppm} 8.53 (broad peak, 2H), 8.08–7.92 (m, 6H), 7.49–7.12 (m, 3H), 2.87 (s, 3H). ^{13}C NMR (101 MHz, DMSO$_{d6}$) δ_{ppm} 160.8, 153.9, 152.9, 147.7, 141.3, 140.3, 135.4, 132.8, 129.7, 129.3, 126.4, 126.0, 125.1, 118.4, 112.3, 108.8, 85.8, 10.5.

Conclusion

In conclusion, we were able to construct Fe$_3$O$_4$@SiO$_2$@DES1 using a straightforward methodology. Instrumental characterization confirmed the successful synthesis and determination of the physicochemical properties of the presented catalyst. The proposed catalyst was used for the synthesis of 1,2,3-triazole-nicotinonitrile hybrids. The free hydroxy groups on the surface of Fe$_3$O$_4$@SiO$_2$ have catalytic activity, and the ionic structure of Ch/Cl can act like an ionic liquid catalyst. Moreover, urea segments act as hydrogen bonding catalysts. These moieties activate the starting materials and intermediates through hydrogen bonding interactions and facilitate the pyridine synthesis reaction. Therefore, the synergistic effects of these parts significantly improve the catalytic potential of Fe$_3$O$_4$@SiO$_2$@DES1, and this hybrid and versatile systems can lead to the activation of different starting materials and intermediates during pyridine synthesis. Besides, due to the heterogeneous nature of Fe$_3$O$_4$@SiO$_2$@DES1, it can be easily separated from the reaction mixture. Thus, desired products were obtained under mild conditions and with high yields. In future studies, this approach can be extended to other catalytic transformations and can be inspiring in chemical studies.

Data availability

The data supporting this article have been included as part of the ESI.†

Conflicts of interest

There are no conflicts to declare.

Acknowledgements

References

1 E. L. Smith, A. P. Abbott and K. S. Ryder, *Chem. Rev.*, 2014, **114**, 11060.

2 B. B. Hansen, S. Spittle, B. Chen, D. Poe, Y. Zhang, J. M. Klein and J. R. Sangoro, *Chem. Rev.*, 2020, **121**, 1232.

3 P. Janicka, M. Kaykhaii, J. Płotka-Wasylka and J. Gębicki, *Green Chem.*, 2022, **24**, 5035.

4 B. Nian and X. Li, *Int. J. Biol. Macromol.*, 2022, **217**, 255.

5 J. Afonso, A. Mezzetta, I. M. Marrucho and L. Guazzelli, *Green Chem.*, 2023, **25**, 59.

6 A. Sanati, M. R. Malayeri, O. Busse and J. J. Weigand, *J. Mol. Liq.*, 2022, **361**, 119641.

7 L. Lomba, M. P. Ribate, E. Sangüesa, J. Concha, M. P. Garralaga, D. Errazquin, C. B. Garcia and B. Giner, *Appl. Sci.*, 2021, **11**, 10061.

8 A. E. Ünlü, A. Arıkaya and S. Takaç, *Green Process. Synth.*, 2019, **8**, 355.

9 G. García, S. Aparicio, R. Ullah and M. Atilhan, *Energy Fuels*, 2015, **29**, 2616.

10 Y. P. Mbous, M. Hayyan, A. Hayyan, W. F. Wong, M. A. Hashim and C. Y. Looi, *Biotechnol. Adv.*, 2017, **35**, 105.

11 Y. Nahar and S. C. Thickett, *Polymers*, 2021, **13**, 447.

12 R. Rodríguez-Ramos, Á. Santana-Mayor, B. Socas-Rodríguez and M. Á. Rodríguez-Delgado, *Appl. Sci.*, 2021, **11**, 4779.

13 A. Monem, D. Habibi and H. Goudarzi, *Sci. Rep.*, 2023, **13**, 18009.

14 P. Liu, J. W. Hao, L. P. Mo and Z. H. Zhang, *RSC Adv.*, 2015, **5**, 4867.

15 J. P. Bittner, N. Zhang, L. Huang, P. D. de María, S. Jakobtorweihen and S. Kara, *Green Chem.*, 2022, **24**, 1120.

16 I. M. Pateli, A. P. Abbott, G. R. Jenkin and J. M. Hartley, *Green Chem.*, 2022, **22**, 8360.

17 X. Yang, Q. Zou, T. Zhao, P. Chen, Z. Liu, F. Liu and Q. Lin, *ACS Sustain. Chem. Eng.*, 2021, **9**, 10437.

18 M. N. T. Tran, X. T. T. Nguyen, H. T. Nguyen, D. K. N. Chau and P. H. Tran, *Tetrahedron Lett.*, 2020, **61**, 151481.

19 W. Jiang, K. Zhu, H. Li, L. Zhu, M. Hua, J. Xiao, C. Wang, Z. Yang, G. Chen, W. Zho, H. Li and S. Dai, *Chem. Eng. J.*, 2020, **394**, 124831.

20 S. E. Hooshmand, R. Afshari, D. J. Ramón and R. S. Varma, *Green Chem.*, 2020, **22**, 3668.

21 A. Triolo, M. E. Di Pietro, A. Mele, F. Lo Celso, M. Brehm, V. Di Lisio and O. Russina, *J. Chem. Phys.*, 2021, **154**, 244501.

22 B. Atashkar, M. A. Zolfigol and S. Mallakpour, *Mol. Catal.*, 2018, **452**, 192.

23 M. Torabi, M. Yarie and M. A. Zolfigol, *Appl. Organomet. Chem.*, 2019, **33**, e4933.

24 P. N. Nguyen, L. H. T. Nguyen, T. L. H. Doan, P. H. Tran and H. T. Nguyen, *RSC Adv.*, 2024, **14**, 7006.

25 P. Makoś-Chełstowska, M. Kaykhaii, J. Płotka-Wasylka and M. de la Guardia, *J. Mol. Liq.*, 2022, **365**, 120158.

26 M. Á. Aguirre and A. Canals, *Trends Anal. Chem.*, 2022, **146**, 11650.

27 (a) M. Bakhtiarian and M. M. Khodaei, *Colloids Surf., A*, 2022, **641**, 128569; (b) M. Zhang, Y. H. Liu, Z. R. Shang, H. C. Hu and Z. H. Zhang, *Catal. Commun.*, 2017, **88**, 39–44.

28 (a) M. Niakan, M. Masteri-Farahani, H. Shekaari and S. Karimi, *Carbohydr. Polym.*, 2021, **251**, 117109; (b) M. H. Zainal-Abidin, M. Hayyan, J. Matmin, A. M. Al-Fakih, N. Jamaluddin, W. M. A. W. Mahmood, R. A. Vahab and F. Abdullah, *J. Ind. Eng. Chem.*, 2023, **124**, 1–16; (c) P. Makoś-Chełstowska, M. Kaykhaii, J. Płotka-Wasylka and M. de la Guardia, *J. Mol. Liq.*, 2022, **365**, 120158.

29 N. Azizi, Z. Rahimi and M. Alipour, *RSC Adv.*, 2015, **5**, 61191.

30 P. H. Tran, *RSC Adv.*, 2020, **10**, 9663.

31 S. Alavinia and R. Ghorbani-Vaghei, *J. Mol. Struct.*, 2022, **1270**, 133860.

32 R. Manujyothi, T. Aneeja and G. Anilkumar, *RSC Adv.*, 2021, **11**, 19433.

33 N. Zarei, M. A. Zolfigol, M. Torabi and M. Yarie, *Sci. Rep.*, 2023, **13**, 9486.

34 B. Saavedra, J. M. Pérez, M. J. Rodríguez-Álvarez, J. García-Álvarez and D. J. Ramón, *Green Chem.*, 2018, **20**, 2151.

35 N. Aziizi, Z. Manochehri, A. Nahayi and S. Torkashvand, *J. Mol. Liq.*, 2014, **196**, 153.

36 M. R. Anizadeh, M. A. Zolfigol, M. Torabi, M. Yarie and B. Notash, *J. Mol. Liq.*, 2022, **364**, 120016.

37 J. Lu, X. T. Li, E. Q. Ma, L. P. Mo and Z. H. Zhang, *ChemCatChem*, 2014, **6**, 2854.

38 J. A. Bull, J. J. Mousseau, G. Pelletier and A. B. Charette, *Chem. Rev.*, 2012, **112**, 2642.

39 C. Allais, J. M. Grassot, J. Rodriguez and T. Constantieux, *Chem. Rev.*, 2014, **114**, 10829.

40 P. Patil, S. P. Sethy, T. Sameena and K. Shailaja, *Asian J. Res. Chem.*, 2013, **6**, 888.

41 C. Wei, Y. He, X. Shi and Z. Song, *Coord. Chem. Rev.*, 2019, **385**, 1.

42 M. Torabi, M. A. Zolfigol and M. Yarie, *Arabian J. Chem.*, 2023, **16**, 105090.

43 G. de Ruiter, M. Lahav and M. E. van der Boom, *Acc. Chem. Res.*, 2014, **47**, 3407.

44 G. Mohammad Abu-Taweel, M. M. Ibrahim, S. Khan, H. M. Al-Saidi, M. Alshamrani, F. A. Alhumaydhi and S. S. Alharthi, *Crit. Rev. Anal. Chem.*, 2022, **54**, 599.

45 R. El-Sayed, *J. Oleo Sci.*, 2015, **64**, 761.

46 G. Tseberlidis, D. Intrieri and A. Caselli, *Eur. J. Inorg. Chem.*, 2017, **2017**, 3589.

47 Y. Wang, Y. Wu, H. Cong, S. Wang, Y. Shen and B. Yu, *J. Polym. Environ.*, 2022, **30**, 385.

48 M. Torabi, M. Yarie, S. Baghery and M. A. Zolfigol, *Recent advances in catalytic synthesis of pyridine derivatives*, Elsevier Inc., 2023, p. 503.

49 Y. Ling, Z. Y. Hao, D. Liang, C. L. Zhang, Y. F. Liu and Y. Wang, *Drug Des., Dev. Ther.*, 2021, **15**, 4289.

50 K. A. Kasabov, N. V. Kudryashov, A. V. Volkova, A. A. Shimshirt, T. S. Kalinina, L. A. Zhmurenko and T. A. Voronina, *Bull. Exp. Biol. Med.*, 2020, **168**, 449.

51 V. K. Sharma, J. M. Hutchison and A. M. Allgeier, *ChemSusChem*, 2022, **15**, e202200888.

52 R. Zafar, H. Naureen, M. Zubair, K. Shahid, M. Saeed Jan, S. Akhtar and A. Sadiq, *Drug Des., Dev. Ther.*, 2021, **15**, 2679.

53 A. E. Mekky and S. M. Sanad, *Synth. Commun.*, 2022, **52**, 2276.

54 R. M. Keshk, G. E. A. Elgawad, E. R. Sallam, M. S. Alsubaie and H. A. Fetouh, *ChemistrySelect*, 2022, **7**, e202202678.

55 S. M. Sanad and A. E. Mekky, *Synth. Commun.*, 2020, **50**, 1468.

56 A. A. El-Sayed, E. A. Elsayed and A. E. G. E. Amr, *ACS Omega*, 2021, **6**, 7147.

57 S. Jalali-Mola, M. Torabi, M. Yarie and M. A. Zolfigol, *RSC Adv.*, 2022, **12**, 34730.

58 M. B. Islam, M. I. Islam, N. Nath, T. B. Emran, M. R. Rahman, R. Sharma and M. M. Matin, *BioMed Res. Int.*, 2023, **2023**, 9967591.

59 J. R. Johansson, T. Beke-Somfai, A. Said Stålsmeden and N. Kann, *Chem. Rev.*, 2016, **116**, 14726.

60 Z. Xu, S. J. Zhao and Y. Liu, *Eur. J. Med. Chem.*, 2019, **183**, 111700.

61 J. P. Wan, S. Cao and Y. Liu, *J. Org. Chem.*, 2015, **80**, 9028.

62 M. Torabi, M. Yarie, M. A. Zolfigol, S. Azizian and Y. Gu, *RSC Adv.*, 2022, **12**, 8804.

63 F. Gao, T. Wang, J. Xiao and G. Huang, *Eur. J. Med. Chem.*, 2019, **173**, 274.

64 R. Kharb, M. Shahar Yar and P. Chander Sharma, *Mini-Rev. Med. Chem.*, 2011, **11**, 84.

65 K. Haider, M. Shafeeque, S. Yahya and M. S. Yar, *Eur. J. Med. Chem. Rep.*, 2022, **5**, 100042.

66 A. Tavassoli, M. Yarie, M. Torabi and M. A. Zolfigol, *J. Phys. Chem. Solids*, 2024, **186**, 111786.

67 (*a*) F. Karimi, M. Torabi, M. Yarie, M. A. Zolfigol and Y. Gu, *J. Iran. Chem. Soc.*, 2023, **20**, 2189; (*b*) N. Zarei, M. Torabi, M. Yarie and M. A. Zolfigol, *Polycyclic Aromat. Compd.*, 2023, **43**, 3072; (*c*) S. Kalhor, M. Yarie, M. Torabi, M. A. Zolfigol, M. Rezaeivala and Y. Gu, *Polycyclic Aromat. Compd.*, 2022, **42**, 4270; (*d*) M. Torabi, M. A. Zolfigol, M. Yarie and Y. Gu, *Mol. Catal.*, 2021, **516**, 111959; (*e*) M. Torabi, M. Yarie, M. A. Zolfigol, S. Rouhani, S. Azizi, T. O. Olomola, M. Maaza and T. A. M. Msagati, *RSC Adv.*, 2021, **11**, 3143; (*f*) H. Sepehrmansourie, M. Mohammadi Rasooll, M. Zarei, M. A. Zolfigol and Y. Gu, *Inorg. Chem.*, 2023, **62**, 9217.

68 (*a*) I. V. Alabugin, L. Kuhn, M. G. Medvedev, N. V. Krivoshchapov, V. A. Vil, I. A. Yaremenko, P. Mehaffy, M. Yarie, A. O. Terent'ev and M. A. Zolfigol, *Chem. Soc. Rev.*, 2021, **50**, 10253; (*b*) I. V. Alabugin, L. Kuhn, N. V. Krivoshchapov, P. Mehaffy and M. G. Medvedev, *Chem. Soc. Rev.*, 2021, **50**, 10212.

69 Y. Bide, M. A. Fashapoyeh and S. Shokrollahzadeh, *Sci. Rep.*, 2021, **11**, 17068.

70 (*a*) M. Yarie, *Iran. J. Catal.*, 2017, **7**, 85–88; (*b*) M. Yarie, *Iran. J. Catal.*, 2020, **10**, 79.

71 M. A. Zolfigol, S. Azizian, M. Torabi, M. Yarie and B. Notash, *J. Chem. Educ.*, 2024, **101**, 877.

72 M. Torabi, M. A. Zolfigol, M. Yarie, B. Notash, S. Azizian and M. M. Azandaryani, *Sci. Rep.*, 2021, **11**, 16846.

73 M. R. Anizadeh, M. Torabi, M. A. Zolfigol and M. Yarie, *J. Mol. Struct.*, 2023, **1277**, 134885.